repulsion leads to a uniform dispersion of the particles. This repulsion arises from a decrease in the configurational entropy of the grafted chain due to the loss of possible configurations, as suggested by Clayfield[16] and Meier[17] and applied to ABS polymers by Moritani et al.[18]

For ABS-3 and ABS-4, the agglomeration of the rubber particles was observed. This is the first observation of agglomerated particles for ABS polymers having high grafting degree, as far as the author knows. It is very interesting to know the reason why the rubber particles are agglomerated at high grafting degree. We speculate as follows, although we can not explain the reason elaborately. For these ABS polymers, D is very much smaller than R_0, and L/D is large. The grafted chains must be stretched strongly. Then, the matrix AS copolymers are expelled from the grafted chains. Phase separation between the matrix and grafted chains is caused and the agglomeration of rubber particles is formed. We are now studying the formation of agglomeration structure at high grafting degree.

Concluding Remarks

In this paper, we reported the effect of grafting degree on the melt viscoelasticity of ABS polymers having particle size of 170 nm. We found that the viscoelastic functions depend strongly on grafting degree in the long-time region associated with particle–particle interactions. As the grafting degree increases, the viscoelastic functions first decrease and then increase. The minima in the functions occurred at the grafting degree of about 0.45. When the grafting degree is below or above 0.45, second-plateau regions in G' and yield stress in the flow curves were observed in long-time region. Transmission electron microscopic observation revealed that rubber particles are finely dispersed for samples having minima in the viscoelastic functions but that the other samples exhibiting second plateaus or yield stresses form an agglomerated or a three-dimensional network structure of rubber particles.

At low grafting degree, the rubber particles cannot form a stable colloid, because the particles are not covered perfectly with grafted chains. The rubber particles also cannot form a stable colloid at high grafting degree, as the matrix chains are expelled from the grafted chains. Only at intermediate grafting degree the particles form stable colloid by the repulsive force between neighboring particles.

Registry No. ABS (graft copolymer), 106677-58-1.

References and Notes

(1) Aoki, Y. *J. Soc. Rheol. Jpn.* **1979**, *7*, 20.
(2) Aoki, Y. *J. Rheol.* **1981**, *25*, 351.
(3) Aoki, Y.; Nakayama, K. *J. Soc. Rheol. Jpn.* **1981**, *9*, 39.
(4) Aoki, Y.; Nakayama, K. *Polym. J.* **1982**, *14*, 951.
(5) Masuda, T.; Nakajima, A.; Kitamura, M.; Aoki, Y.; Yamauchi, N.; Yoshioka, A. *Pure Appl. Chem.* **1984**, *56*, 1457.
(6) Aoki, Y. *J. Non-Newt. Fluid Mech.* **1986**, *2*, 91.
(7) Zosel, A. *Rheol. Acta* **1972**, *11*, 229.
(8) Moroni, A.; Casale, A. *Proc. Int. Rheol. Congr. 7th* **1976**, 339.
(9) Huguet, M. G.; Paxton, T. R. *Colloidal and Morphological Behavior of Block and Graft Copolymers*; Plenum: New York, 1971; p 183.
(10) Münstedt, H. *Polym. Eng. Sci.* **1981**, *21*, 259.
(11) Krieger, I. M.; Maron, S. H. *J. Appl. Phys.* **1952**, *23*, 147.
(12) Cox, W. P.; Merz, E. H. *J. Polym. Sci.* **1958**, *28*, 619.
(13) Casson, N. *Rheology of Disperse Systems*; Pergamon: New York, 1959.
(14) Kato, K. *J. Electron Microsc.* **1965**, *14*, 220.
(15) de Gennes, P.-G. *Macromolecules* **1980**, *13*, 1075.
(16) Clayfield, E. J.; Lumb, E. C. *J. Colloid Interface Sci.* **1966**, *22*, 269.
(17) Meier, D. J. *J. Phys. Chem.* **1967**, *71*, 1861.
(18) Moritani, M.; Inoue, T.; Motegi, M.; Kawai, H. *Macromolecules* **1970**, *3*, 433.

Interactions in Mixtures of Poly(ethylene oxide) and Poly(methyl methacrylate)

H. Ito and T. P. Russell*

IBM Research, Almaden Research Center, San Jose, California 95120-6099

G. D. Wignall

Oak Ridge National Laboratory, Solid State Division, Oak Ridge, Tennessee 37830.

Received April 20, 1987

ABSTRACT: Small-angle neutron-scattering measurements have been performed on mixtures of poly(ethylene oxide), PEO, with protio- and deuteriopoly(methyl methacrylate), PMMAH and PMMAD, respectively, to evaluate the Flory–Huggins interaction parameter χ_{AB}. It has been found that χ_{AB} varies from -5×10^{-3} to -1×10^{-3} as the total PMMA concentration increases from 0.3 to 0.7. The temperature dependence of the scattering combined with other results indicates that entropic, rather than enthalpic, contributions dominate χ_{AB}. The magnitude of χ_{AB} is found to be on the same order of magnitude as that expected between PMMAH and PMMAD, particularly at high total concentrations of PMMA. Studies of PMMA at higher scattering vectors show that down to length scales of 25 Å no changes are observed in the conformation of PMMA in the mixtures in comparison to that of PMMA in the bulk.

Introduction

The binary interaction parameter in the free energy of mixing is critical for the evaluation of the miscibility between polymer pairs. In principle, the determination of the interaction parameter, χ, is possible by a variety of techniques. However, in practice, obtaining a precise value of χ is not trivial. Melting point depression studies have been used in the past to determine χ for semicrystalline/amorphous polymer pairs.[1] For some systems this method has been used with a fair degree of success. Use of the melting point depression technique requires the measurement of the equilibrium melting point, T_m^0 of the pure semicrystalline polymer and of the semicrystalline polymer in the mixture. By no means is this a simple and clear-cut measurement. Lamellar thickening during heating, modification of the crystal structure, and super-

0024-9297/87/2220-2213$01.50/0

heating of the crystal during heating can present problems. Even without these problems this method requires the extrapolation of the measured melting points over a relatively large temperature range to determine T_m^0. The errors introduced by this extrapolation can, in some cases, obscure any depression in T_m^0 due to specific interactions. Ternary solution theory can also be used to evaluate χ. Measurement of the heats of mixing of the binary solutions of the homopolymers in a common solvent and the heat of mixing of a ternary solution of the two polymers in the same solvent will yield the polymer/polymer interaction parameter.[2] Similarly, inverse chromatographic techniques can be utilized to extract χ.[3] These methods, however, assume that the polymer/polymer interaction parameter is not altered by the presence of a solvent. Polymer/polymer interdiffusion has recently emerged as being a very sensitive means by which to evaluate χ.[4,5] While this technique has been quite successful, it is rather specialized. At present, ion beam spectrometers are not available to most experiments, thereby making the realization of the experiments difficult.

An alternative to these techniques is either small-angle X-ray scattering (SAXS) or small-angle neutron scattering (SANS). Wendorff et al.[6] clearly demonstrated the utility of SAXS for the measurement of χ for mixtures of poly(vinylidene fluoride) with poly(methyl methacrylate). SAXS, however, requires that the electron density differences between the two polymers be large enough to yield a detectable level of scattering. SANS, on the other hand, circumvents this problem when one of the components is isotopically labeled with deterium. Several studies have appeared in the literature, treating the scattering from multicomponent systems and more specifically from binary mixtures, where the SANS can be split into terms arising from intramolecular and intermolecular correlations.[7,8,9] χ can then be evaluated from the intermolecular component of the scattering. If χ is not too negative, SANS affords a simple and accurate means of measuring χ.

The mixture of interest in this study is that of poly(ethylene oxide), PEO, and poly(methyl methacrylate), PMMA. In a recent investigation of the crystallization kinetics in these mixtures a theoretical treatment was presented that reasonably described the experimentally observed growth rates.[10] A critical assumption made in this study was that $\chi \simeq 0$ for this mixture. Attempts to evaluate χ by melting point depression studies were not possible due to the problems mentioned above. In this article, the measurement of χ for PEO and PMMA by SANS is discussed. It is shown that the value of χ for PEO and PMMA is quite small and depends upon composition. In fact, the magnitude of χ for PEO and PMMA is shown to be comparable to that typically observed for mixtures of chemically identical but isotopically different polymers. In addition, the conformation of PMMA in the bulk homopolymer and in the mixtures is discussed.

Experimental Section

Synthesis of PMMA. Perdeuteriated methyl methacrylate (MMAD, 99.3 atom % D) purchased from Merck, was first dried over CaH_2, distilled under high vacuum, then further dried by titrating with a Et_3Al solution in hexane (Aldrich),[11] and distilled 3 times under high vacuum with the center cut being taken each time. The purified monomer was distributed by distillation in vacuo into calibrated glass ampules connected to break seals and stored in liquid nitrogen.

Dried and distilled *n*-butyl bromide (1.40 g, 1.02×10^{-1}/mol) was reacted with lithium (0.146 g) in dry *n*-hexane under high vacuum with use of a break-seal technique to form a 0.51 M solution of *n*-butyllithium (*n*-buLi). Lithium bromide produced in the reaction was filtered away in the apparatus sealed under high vacuum. (1,1-Diphenylhexyl)lithium solution (DPHLi, 0.1 M) was prepared by reacting *n*-BuLi with dry 1,1-diphenylethylene in *n*-hexane and distributed into calibrated tubes connected to a break seal by turning the apparatus upside down. All the reagents were handled under high vacuum.

Table I
Characterization of Polymers Used

polymer	M_w[a]	M_w/M_N	M_{mon}[b]
poly(ethylene oxide)	145 000	1.03	44
deuteriopoly(methyl methacrylate)	129 000	1.05	108
protiopoly(methyl methacrylate)	125 000	1.05	100

[a] Weight-average molecular weights were determined by solution light scattering. [b] M_{mon} is the molecular weight of the repeating unit.

Transfer of all the reagents and polymerization were carried out under high vacuum with use of a break-seal technique. The DPHLi solution (0.125 mL, 0.1 M) was introduced into a polymerization ampule and diluted with tetrahydrofuran (THF, 10.0 mL) which had been refluxed over sodium metal, distilled, and then finally dried on a sodium mirror under high vacuum. After melting the initiator and solvent ampules off, the polymerization apparatus connected to an ampule containing the monomer solution (20 mL) in THF (10.0 mL) was melted off the vacuum line. The initiator solution was maintained at −78 °C, to which was slowly added the cooled monomer solution. The polymerization mixture was vigorously agitated while the monomer solution was flowing into the polymerization ampule. After the mixture was allowed to stand at −78 °C for 1–3 h, the contents were frozen, the ampule was cut open, cold methanol containing a small amount of acetic acid was added to the mixture, and the contents were mixed thoroughly while being thawed at −78 °C. The resulting solution was poured in stirred methanol to precipitate the polymer. After filtration, the polymer was dried overnight at ca. 60 °C in a vacuum oven. The yield was quantitative. The tacticity of the deuteriated polymer was determined by 50-MHz ^{13}C NMR in deuteriochloroform at room temperature. Molecular weights were measured by size exclusion chromatography in THF with polystyrene as a standard and, also, by low-angle light scattering on solutions in toluene.

Neutron-Scattering Measurements. The characteristics of the polymers used in this study are given in Table I. The poly(ethylene oxide) PEO, purchased from Polymer Laboratories, is a calibration standard for aqueous size exclusion chromatography (TSK Standard PEO produced by Toyo Soda Manufacturing Co., Ltd.) and had an $M_w = 145\,000$ with an $M_w/M_n = 1.03$. The protiopoly(methyl methacrylate), PMMAH, purchased from Polymer Laboratories, had an $M_w = 125\,000$ with $M_w/M_n = 1.05$. The deuteriopoly(methyl methacrylate), PMMAD, synthesized as described above, had an $M_w = 129\,000$ with $M_w/M_n = 1.05$. All polymers were used as received without further purification and were dried under vacuum at 40 °C overnight prior to use. Samples for neutron-scattering measurements were prepared by dissolving preweighed, dry mixtures of PMMAH, PMMAD, and PEO in benzene at 35 °C. After complete dissolution of the components, the solutions were frozen in liquid nitrogen, transferred to an ice water bath and freeze-dried. Upon removal of the benzene, the diaphanous powder was transferred to a vacuum oven, dried for 48 h at 50 °C, and dried for another 48 h at a temperature 10 °C below the glass transition temperature of the mixture or 10 °C below the melting point of the PEO in the mixture. Initially, the powders were pressed in a pellet mold at room temperature and then melt pressed at 130 °C in circular molds 1.3 cm in diameter and 0.1 cm in thickness. Both visual observation and small-angle X-ray scattering indicated that the samples were free of voids.

The molded disks were placed into scattering cells consisting of a Teflon washer, designed to match the sample disks, and two circular quartz windows. These were placed into brass holders constructed to accommodate samples of varying thicknesses and to fit within the heating chamber at the National Center for Small Angle Scattering Research (NCSASR) at the Oak Ridge National Laboratory. A description of the facility has recently been given by Koehler.[12] A set of five specimens at a given total concentration of PEO but varying in the PMMAH/PMMAD ratios were mounted into the heated automatic sample changer which was

purged with helium. The temperature was controlled at 80 ± 0.2 °C with a Laude recirculating temperature bath. Approximately 20 min were allowed for the specimens to come to thermal equilibrium prior to initiating measurements. Use of this sample changer introduced two additional single-crystal silicon windows forming the seal between the helium atmosphere and a vacuum of the scattering apparatus. The contributions of these to the observed scattering was negligible.

SANS measurements were performed at sample to detector distances of 14.98, 4.99, and 1.38 m with beam guides being used at the shorter distances to enhance the flux on the specimen. A 1-cm-diameter cadmium slit directly before the sample and either a 1.0- or 1.3-cm-diameter slit at the source collimated the incident neutron beam. All measurements were conducted with neutrons of wavelength $\lambda = 4.75$ Å having a $\Delta\lambda/\lambda$ of 0.06. The scattering profiles were placed on an absolute level by using a series of previously calibrated standards, namely, a calibrated aluminum standard, a protio- and deuteriopolystyrene mixture, and protiopolystyrene dissolved in deuteriobenzene.[13] The scattering profiles were scaled to the 15-m data by using factors of 0.20 ± 0.001 for the 5-m data and 0.040 ± 0.002 for the 1.38-m data. These factors corresponded to geometric factors taking into account the changes in the scattering volume and in the solid angle subtended by each detector element. Transmission factors of samples were measured at room temperature and were found to be within ±3% of the value calculated from the formula $T = \exp(-t\sum_i N_i\sigma_i^T/V)$ where σ_i^T is the total scattering cross section of monomer i with number fraction N_i, t is the sample thickness, and V is the volume.

Mixtures of PEO and PMMA were prepared at PEO monomer fractions 1.0, 0.70, 0.50, 0.25, and 0. At each of these concentrations five different samples were investigated where the number fraction of the PMMAD was varied from 0 to 1. Evaluation of the absolute coherent scattering cross section $[(d\Sigma/d\Omega)(q)]$ for these mixtures requires the elimination of the incoherent scattering and the coherent thermal density fluctuation scattering. q in this term is the scattering vector given by $q = (4\pi/\lambda)\sin(\epsilon/2)$ where λ is the wavelength of the incident radiation and ϵ is the scattering angle. In a manner analogous to that of Hayashi et al.,[14]

$$\left[\frac{d\Sigma}{d\Omega}(q)\right] = \left[\frac{d\Sigma}{d\Omega}(q)\right]_m - C_1\left[\frac{d\Sigma}{d\Omega}(q)\right]_{PEO} - C_2\left[\frac{d\Sigma}{d\Omega}(q)\right]_{PMMAH,inc} - \left(\frac{\bar{a}}{a_D}\right)^2\left[\frac{d\Sigma}{d\Omega}(q)\right]_{PMMAD} \quad (1)$$

where $[d\Sigma/d\Omega)(q)]_i$ is the measured absolute scattering of component i (m indicates the mixture of interest), a_D is the coherent scattering length of PMMAD, and $\bar{a}$ is the average scattering length of the PMMA in the mixtures. $\bar{a}$ is given by $\sum_i x_i a_i$ where x_i is the number fraction of monomer i with coherent scattering length a_i. The incoherent scattering of PMMAH is given by

$$\left[\frac{d\Sigma}{d\Omega}(q)\right]_{PMMAH,inc} = \left[\frac{d\Sigma}{d\Omega}(q)\right]_{PMMAH} - \frac{t_H T_H \sigma_{H,coh}}{t_D T_D \sigma_{D,coh}}\left[\frac{d\Sigma}{d\Omega}(q)\right]_{PMMAD} \quad (2)$$

where $\sigma_{H,coh}$ and $\sigma_{D,coh}$ are the coherent cross sections of PMMAH and PMMAD, respectively, with thickness t and transmission factors T. The coefficients C_1 and C_2 are given by

$$C_1 = \frac{1 - \exp(-N_{PEO,m}\sigma_{PEO}t_m)}{1 - \exp(-N_{PEO}\sigma_{PEO,inc}t_{PEO})} \quad (3a)$$

and

$$C_2 = \frac{1 - \exp(-N_{PMMAH,m}\sigma_{PMMAH}t_m)}{1 - \exp(-N_{PMMAH}\sigma_{PMMAH,inc}t_{PMMAH})} \quad (3b)$$

where $N_{i,m}$ is the number of monomers per unit volume of component i in the mixture with thickness t_m, N_i is the number of monomers per unit volume of component i in the mixture that are fully protonated, and $\sigma_{i,inc}$ is the incoherent scattering cross section of component i.

At this point it is worth noting that the incoherent scattering does not contribute significantly to the scattering at smaller scattering vectors or, in other words, small errors in the incoherent scattering will not affect the scattering used to evaluate χ. However, at larger scattering vectors where the total scattering is small and is comparable to the incoherent scattering, small errors in the level of the incoherent scattering can severely limit quantitative interpretation of the data.

Table II
Characteristics of PMMA[a]

	protio	deuterio		protio	deuterio
triad sequences			diad content		
% rr	54	73	% r	75	86
% mr	43	26	% m	25	14
% mm	3	1			

[a] m and r indicate meso and racemic, respectively.

Results and Discussion

SANS measurements on mixtures of PEO and PMMA provide a means of evaluating not only the interaction parameter betwen these two polymers but also the conformation of the PMMA in the bulk and in the mixtures. It is worthwhile to concentrate first on the PMMA homopolymers for several reasons. First, both the protio and deuterio polymers studied here have narrow molecular weight distributions. Most studies to date have dealt with polydisperse materials and, as such, the polymers prepared in this work provide a unique means of probing both local and global characteristics of this polymer in the absence of polydispersity effects. Second, the polymers prepared in this work cannot be considered "strictly" atactic polymers. Synthesis of narrow molecular weight distribution polymers requires the use of low temperatures and the tacticity of this polymer may be different from PMMA studied by others. Data on the tacticity of the protonated and deuteriated PMMA used in this study are given in Table II. As can be seen, the two polymers are very closely matched. These data must be considered when comparing the results in this study with other published data.

PMMA Homopolymer. A series of five different mixtures of protio and deuterio PMMA were investigated with the number fraction of PMMAD varying from 0 to 1. Scattering measurements were performed at 80 °C to be consistent with the measurements of the PEO/PMMA mixtures. This, however, is some 35 °C below the glass transition temperature of the PMMA. Evaluation of the single-chain structure factor in concentrated H/D mixtures has been discussed by numerous authors[15-19] and will not be reiterated here. The most important assumptions made in these arguments is that the H/D mixtures are incompressible and the interaction parameter between the protonated and deuteriated polymers, χ_{HD}, is zero. While the former assumption is reasonable it has recently been shown that χ_{HD} is not zero.[20-23] This will be discussed in more detail later.

By use of modified versions of eq 1 and 2 the absolute coherent elastic scattering, $[(d\Sigma/d\Omega)(q)]$, was determined for the different H/D mixtures. These were normalized by the product $\phi_H(1 - \phi_H)$ where ϕ_H is the volume fraction of the protonated polymer and $(a_H - a_D)^2$ where a_i is the coherent scattering cross section of component i. The results of this analysis for the three different H/D mixtures are shown in Figure 1. It is evident that the normalizations mentioned reduced the data from the different H/D mixtures to one curve.

These data were analyzed according to a Zimm analysis to evaluate the molecular weight and radius of gyration. Zimm plots for the reduced single-chain scattering are shown in Figure 2. Linearity in the Zimm plots were seen up to values of q^2 of 6×10^{-4} Å^{-2} ($q = 0.024$ Å^{-1}) whereupon pronounced deviations were found. The results of the

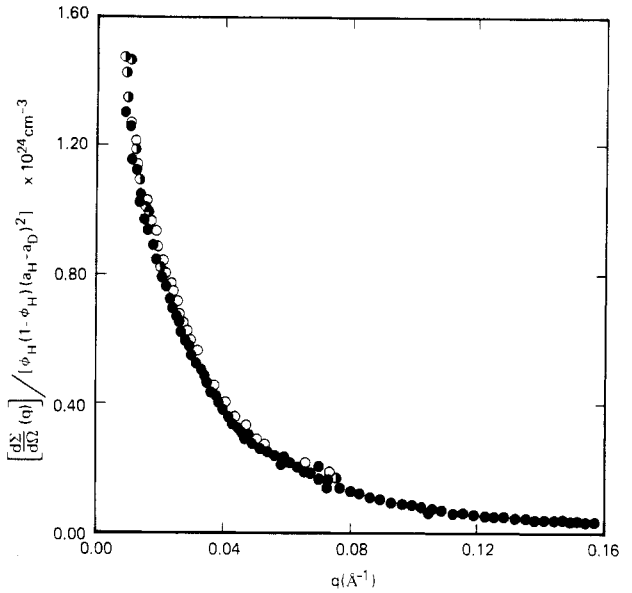

Figure 1. Elastic, coherent small-angle neutron scattering for mixtures for mixtures of PMMAH and PMMAD in the bulk state. The symbols correspond to PMMAD monomer fractions of (○) 0.3, (●) 0.5, and (◑) 0.75.

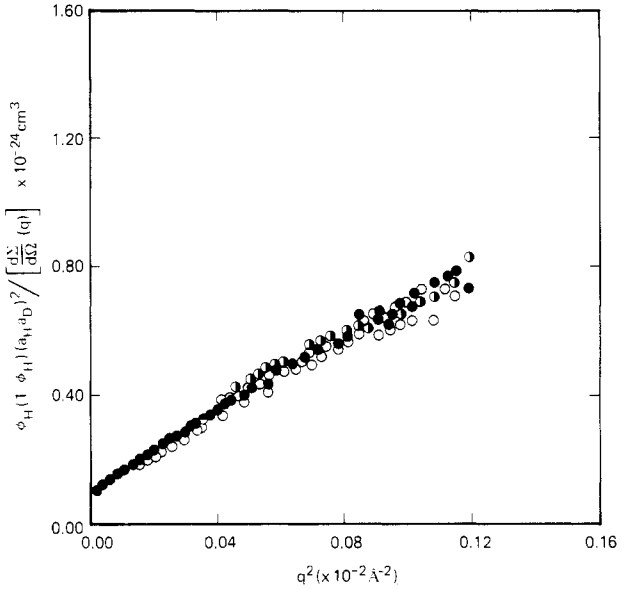

Figure 2. Zimm plots of the single-chain structure factor of PMMA. The symbols correspond to PMMAD fractions of (○) 0.3, (●) 0.5, and (◑) 0.75.

Table III
Results of Zimm Analysis

ϕ_{PMMA}	$X_{PMMA,H}$	$M_w \times 10^{-3}$	Rg, Å
1.0	0.25	133	104
1.0	0.50	139	103
1.0	0.75	136	105
0.74	0.21	130	91
0.74	0.52	117	108
0.74	0.81	123	99
0.48	0.21	129	110
0.48	0.52	137	115
0.48	0.81	136	112
0.30	0.52	133	117

Zimm analysis are shown in Table III, taking into account corrections due to the angular range over which the analysis was performed as discussed by Ullman.[24] Of interest here are the results in the first three rows corresponding to total volume fractions of PMMA (both protonated and deuteriated) of one. On average a weight-average molecular weight, M_w, of 136 000 with a radius of gyration, R_g, of 104 Å was found. The molecular weight compares quite well to values of 129 000 determined by low-angle light scattering and 136 300 by size-exclusion chromatography. Thus, it is apparent that the two polymers are segmentally intermixed and there is no evidence of clustering. The radius of gyration compares well to values of R_g reported by Dettenmeier et al.[25] and by O'Reilly et al. for atactic PMMA with a meso diad content of ca. 20%.[26]

The characteristic ratio, C_n, is defined by[27]

$$C_n = (6R_g^2/M)(m_g/l^2) \quad (4)$$

where m_b is the molecular weight per skeletal bond of length l. For PMMA,[28] $m_b = 50$ and $l = 1.53$ Å. For the values of R_g and M_w reported here, $C_n = 9.8$ which compared to values of 9.2 reported by O'Reilley et al.[27] for syndiotactic-rich PMMA. Typical values of C_n for atacitic PMMA where the meso diad content is ca. 20% range from 7.3 as reported by Jenkins and Porter[29] to 8.3 as found by Dettenmeier et al.[25] Comparison of values of C_n for PMMA must, however, be done with caution. Since the conformation of the molecule depends strongly on the tacticity of the chain, C_n will vary with the meso diad content. In addition, errors in both M_w and R_g can hamper a meaningful comparison of C_n.

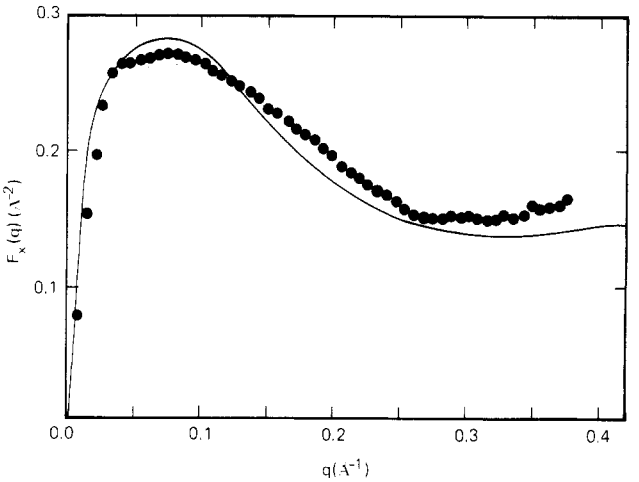

Figure 3. Absolute Kratky plot of PMMA corresponding to the average of the single-chain structure factor obtained from PMMAD monomer fractions of 0.3, 0.5, and 0.75. The solid line corresponds to recent results of Dettenmeier et al.[25]

The single-chain scattering at intermediate angle reflects the conformation of the individual PMMA molecules. Both experimental[25,26,30-33] and theoretical[28,34-36] studies on the conformation of PMMA in solution and in the bulk state have been published. In Figure 3 is shown an absolute Kratky plot of the single-chain scattering obtained in this study. In this figure $F_x(q)$ is given by

$$F_x(q) = q^2\left[\frac{d\Sigma}{d\Omega}(q)\right] m_D/\phi_H(1-\phi_H)(a_H - a_D)^2 N_A \quad (5)$$

where m_D is the molecular weight of the deuteriated monomer unit and N_A is Avogadro's number. It has been assumed that the PMMA is fully deuteriated. Incomplete deuteriation will effectively reduce the contrast difference and increase $F_x(q)$. Along with these data is shown a solid curve that corresponds to recent results of Dettenmeier et al.[25] As can be seen the data from these two studies, given the differences in the molecular weights, are in very good agreement out to relatively high scattering vectors. The agreement at the higher scattering vectors is surprising

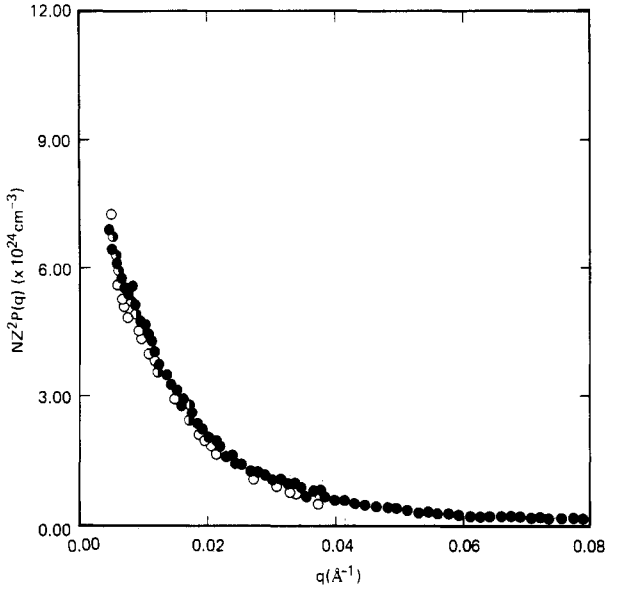

Figure 4. Intramolecular scattering function of PMMAD in a 50/50 mixture of PMMA/PEO. The individual symbols correspond to PMMAD monomer fractions of (○) 0.25, (●) 0.5, and (◑) 0.75.

since relatively small changes in the incoherent scattering can substantially alter $F_x(q)$. The results of these two studies are, also, in agreement with the rotational isomeric state calculations of Yoon and Flory.[34,35] Precise comparison with these theoretical calculations cannot be made due to the differences in the meso diad contents of the polymers studied here and that used in the calculations. However, the dominant feature of $F_x(q)$, namely, the pronounced maximum at $q = 0.08$ Å^{-1}, is clearly evident. It is also clear that PMMA cannot be approximated by a Debye coil at scattering vectors greater than 0.06 Å^{-1} since $F_x(q)$ continually decreases. For a Debye coil, of course, $F_x(q)$ would be constant at these higher scattering vectors.

PEO/PMMA Mixtures. In order to extract the single-chain structure factor from the scattering of a polymer mixture it is necessary to use a ternary mixture comprised of homopolymer A, protonated homopolymer B, and deuteriated homopolymer B. By keeping the total ratio of A to B constant and varying the ratio of protonated B to deuteriated B, it has been shown by several authors[7-9,37] that the single-chain characteristics of component B can be determined. Essentially the total scattering is divided into an intramolecular component, $P(q)$, and an intermolecular component, $Q(q)$. By assuming that the mixture is incompressible, that $\chi_{HD} = 0$, and that $Q_{HD}(q) = Q_{DD}(q) = Q_{HH}(q)$, the total elastic coherent scattering cross section measured is given by

$$[(d\Sigma/d\Omega)(q)] = x(1-x)(a_D - a_H)^2NZ^2P(q) + (\bar{a} - a_A)^2NZ^2[P(q) + NQ(q)] \quad (6)$$

where x is the number fraction of molecules of type B (in this case, PMMA) that are deuteriated, Z is the degree of polymerization, N is the total number of polymers of type B per unit volume, and a_A is the coherent scattering length of component A (here, PEO). The average scattering length of component B is given by

$$\bar{a} = xa_D + (1-x)a_H \quad (7)$$

It has also been assumed that the only difference between the H and D molecules is the isotopic labeling. In particular, the degrees of polymerization and the tacticities of the H and D polymers are assumed identical. For the PMMAH and PMMAD used in this study $Z_H = 1250$ and $Z_D = 1259$, thereby making this assumption of identical

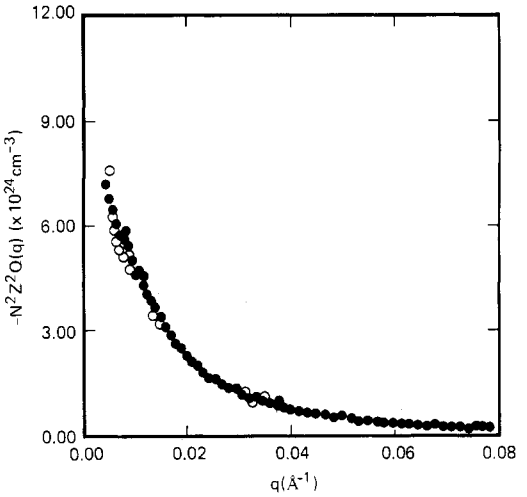

Figure 5. Intermolecular scattering function of PMMAD in a 50/50 mixture of PMMA/PEO. The individual symbols correspond to PMMAD monomer fraction of (○) 0.25 and (●) 0.50. The data for the 0.75 PMMAD monomer fraction is indistinct from those of the other compositions.

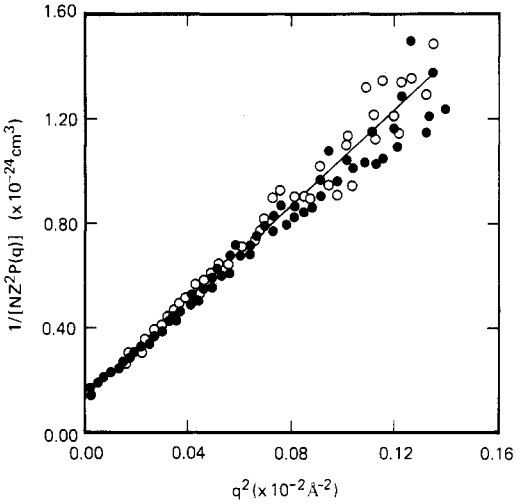

Figure 6. Zimm plots of the intramolecular scattering function of PMMAD in a 50/50 mixture of PMMA/PEO. The data shown correspond to PMMAD monomer fractions of (○) 0.25 and (●) 0.5.

molecular weights quite reasonable. There are slight differences in the tacticities of the two polymers which may invalidate the assumption that $P_H(q) = P_D(q)$. However, these differences were not evident in the H/D studies on pure PMMA discussed previously.

In this study, total PMMA volume fractions of 0.30, 0.48, and 0.75 were investigated. For each of these concentrations the total number fraction of PMMAD was varied from 0 to 1 with three intermediate H/D compositions. Thus, for each total composition of PMMA, eq 6 can be solved simultaneously for the different H/D compositions in order to determine $P(q)$ and $Q(q)$. For example, in Figures 4 and 5 are shown plots of $NZ^2P(q)$ and $-N^2Z^2Q(q)$, respectively, determined by three different combinations of the scattering from the different H/D mixtures where the total volume fraction of PMMA was kept constant at 0.48. The superpositioning of both the intermolecular and intramolecular scattering functions, as can be seen, was found to be quite good. Similar superpositioning was found for the other total compositions of PMMA.

The intramolecular scattering function can be analyzed in the usual Zimm manner to obtain the radius of gyration and molecular weight of the PMMA. In Figure 5 the

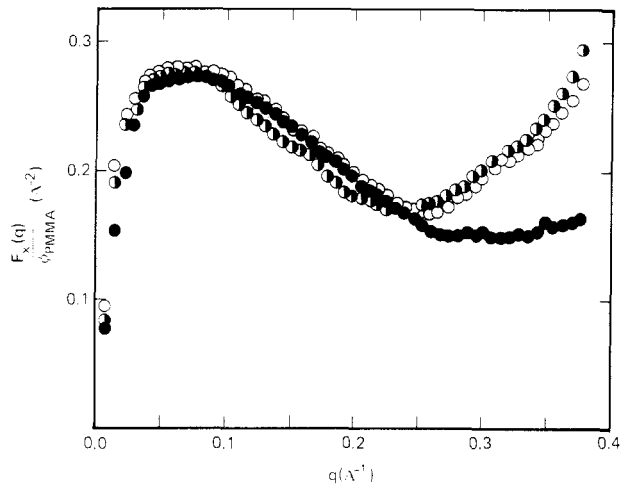

Figure 7. Absolute Kratky plots for total PMMA monomer fractions of (○) 1.0, (●) 0.5, and (◑) 0.30. The data for the 0.75 PMMAD monomer fraction is not shown. For each composition at least three different determinations of $NZ^2P(q)$ were averaged together. Normalization of the data by ϕ_{PMMA} was necessary to account for the reduction in the total signal arising from PMMA due to the presence of PEO.

inverse of the intramolecular scattering function, shown in Figure 4, is plotted as a function of q^2. The results of the Zimm analysis for each of the mixtures investigated are given in Table III. It is seen from these data that, to within experimental errors, the molecular weight of the PMMA remains constant as the total concentration of PMMA varies. These data are also consistent with the molecular weights obtained for the pure PMMA H/D mixtures. This is strong evidence that PEO and PMMA are segmentally mixed and that at 80 °C, the temperature of the measurements, PEO and PMMA, are miscible. The data in Table III also show that the radius of gyration of the PMMA does not change significantly. At the higher PEO concentrations there appears to be a slight increase in the R_g; however, this is at the limit of experimental errors and cannot be considered significant.

Having determined the intramolecular scattering function, any changes in the molecular conformation of PMMA due to specific interactions with the PEO can be deduced by examining an absolute Kratky plot. In Figure 7 are shown plots of $F_x(q)$ vs. q for the different PMMA concentrations studied along with that of the pure PMMA. It should be noted that $F_x(q)$ was normalized by the total volume fraction of PMMA; i.e., the $F_x(q)$ in Figure 7 is actually $F_x(q)/\phi_{PMMA}$ where ϕ_{PMMA} is the volume fraction of PMMA. Division by ϕ_{PMMA} is necessary since there is a loss in scattering arising from PMMA due to the presence of PEO. As can be seen from these data, $F_x(q)$ for PMMA does not change significantly for these mixtures up to a scattering vector of ca. 0.25 Å^{-1}. At higher scattering vectors pronounced deviations of the single chain structure factor of the PMMA in the mixtures from that in pure PMMA are seen. Unfortunately due to low level of total scattering in comparison to the magnitude of the incoherent scattering a quantitative assessment of these differences is difficult. In addition, the slight tacticity differences between the H and D polymers may be giving rise to the observed differences.

All information relevant to the magnitude and sign of the Flory–Huggins interaction parameter is contained in $Q(q)$. In particular,

$$\chi_{AB} = [[\phi Z_A(P(0) + NQ(0))]^{-1} - (\phi_A Z_A)^{-1} - ((1 - \phi_A)Z_B)^{-1}]/2 \quad (8)$$

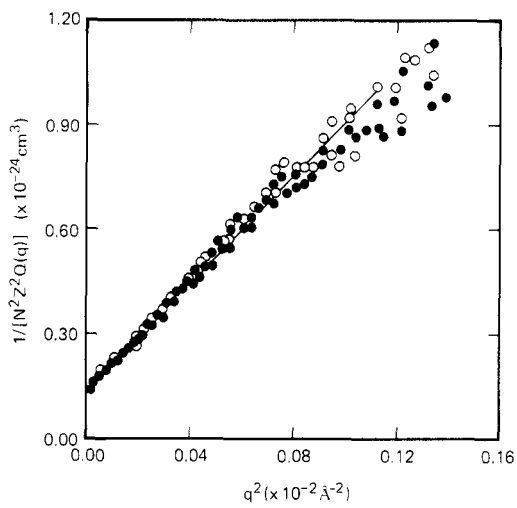

Figure 8. Zimm plots of the intermolecular scattering function for a 50/50 mixture of PMMA/PEO. Data for PMMAD monomer fractions of 0.25 (○) and 0.5 (●) are shown. These plots were used specifically to evaluate $-N^2Z^2Q(q)$ at $q = 0$.

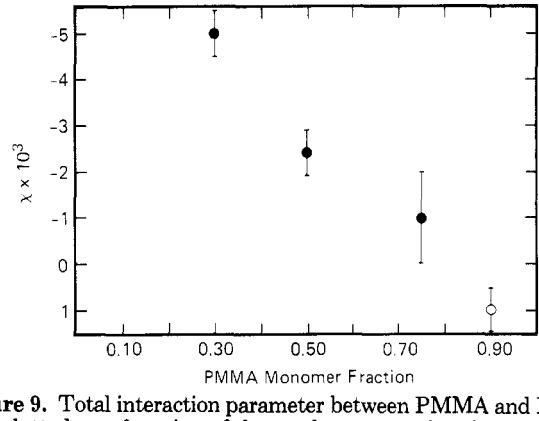

Figure 9. Total interaction parameter between PMMA and PEO, χ_{AB}, plotted as a function of the total monomer fraction (H + D) of PMMA. The open circles are the data of Lefebvre et al.[38]

Since $P(0) = 1$ and the characteristics of both the polymers in the mixtures, i.e., Z_A,Z_B and ϕ_A, are known, then determination of $Q(q)$ at $q = 0$ yields the Flory–Huggins interaction parameter χ_{AB} directly. A reasonable assumption for the functional form of $Q(q)$ is an expontential in q^2. Thus, at small values of q, a Zimm type of analysis should be applicable. For the $Q(q)$ data of the $\phi_{PMMA} = 0.48$ mixture shown in Figure 5, the plot of $Q(q)^{-1}$ vs. q^2, shown in Figure 8, was obtained. As with the Zimm plots for $P(q)$ linearity of the plots were seen for $q^2 \lesssim 6 \times 10^{-3}$ Å^{-2} whereupon the data began to deviate from the Zimm or exponential behavior. However, reasonable extrapolations to $q = 0$ were possible.

The Flory–Huggins interaction parameters for the PEO/PMMA mixtures were obtained at the three different compositions and are plotted in Figure 9 as a function of the monomer fraction of PMMA in the mixture. There are several features of these data that are striking. First, the magnitude of χ_{AB} for the PEO/PMMA mixture is quite small. In fact, based on the results of other studies χ_{AB}, at higher PMMA concentrations, is comparable to that expected from the interactions between protio and deuterio PMMA. This point will be discussed in more detail later. Second, there is a clear concentration dependence of χ_{AB}. In fact, χ_{AB} is negative for low PMMA concentrations and increases to near zero at PMMA monomer fraction of 0.75. Independent studies of Lefebvre et al.[38] on similar mixtures yielded a value of χ_{AB} at 0.9 monomer fraction of PMMA of 1×10^{-3}. This result

corresponds to the open circle in Figure 9. As can be seen, the value of χ_{AB} obtained in their study fit quite well with the values of χ_{AB} obtained here. These combined results suggest that χ_{AB} varies from negative to positive values as the concentration of PMMA increases. This would indicate that enthalpic contributions to χ_{AB} may be dominated by the entropic contributions. If this were not the case then it would be difficult to account for the changing of sign in χ_{AB}. Measurements of the temperature dependence of χ_{AB} showed that for a PMMA monomer fraction of 0.74, over an 80 °C temperature range, the value of χ_{AB}, to within experimental errors, remained constant.[39] Dominance of χ_{AB} by enthalpic contributions would be indicated by a strong temperature dependence. The invariance of the scattering with temperature indicates that the entropic contributions to χ_{AB} are more important. Theoretical arguments of Bawendi and Freed[40] have shown that if the degrees of polymerization of the two polymers are different then a composition dependence of an interaction parameter based strictly on entropic contributions is expected. Their calculations based on a lattice model yield

$$\frac{\partial \chi_{AB}}{\partial \phi_B} = -\frac{12}{z^2}\left(\frac{1}{D_A} - \frac{1}{D_B}\right) \tag{9}$$

where z is the coordination number of the lattice and D_i is the number of statistical segments comprising polymer i. D_i will be a constant K times the degree of polymerization. According to these authors, these values will be $K \simeq 4$ and $Z \approx 6$. Therefore, $\partial\chi_{AB}/\partial\phi_B \approx 6.6 \times 10^{-4}$. The value determined experimentally is 8.9×10^{-3} in reasonable agreement with their prediction. Theoretically, however, the crossover between positive and negative values of χ_{AB} should occur at a volume fraction of 0.5. Experimentally, this is not found which may reflect slight enthalpic contributions to χ_{AB}. Regardless of the origins of χ_{AB} it is clear from these results that χ_{AB} is quite small, which is in keeping with an assumption made previously in a study of the crystallization of these mixtures.

From the values of χ_{AB} determined in this study the melting point depressions for mixtures of PEO and PMMA can be calculated. At a volume fraction of PMMA of 0.5 a melting point depression of approximately 5 °C is found. This small depression of the melting point can easily be obscured by problems mentioned previously in the introduction. Therefore, the previous observation that the melting point depression for the PEO/PMMA mixtures was small[10] is fully consistent with the results of this work.

Magnitude of the Interaction Parameter. Since the magnitude of χ_{AB} is quite small a question that arises is whether or not the assumption that $\chi_{HD} = 0$ is reasonable. Direct calculation of χ_{HD} is not possible. However, an estimation of χ_{HD} based on a carbon to hydrogen ratio can be made from the χ_{HD}'s measured for other polymers.[21-23,41] For example, for polystyrene with a C:H ratio of 1:1 χ_{HD} is found to be 1.7×10^{-4} whereas for polybutadiene with a C:H ratio of 2:3 χ_{HD} is 5.2×10^{-4}. PMMA, counting the oxygens as carbon atoms, has a C + O:H ratio of 7:8 and, therefore, a value of $\chi_{HD} \simeq 2.0 \times 10^{-4}$ would be predicted. Since χ_{AB} ranges from 1.0 to -5.0×10^{-3}, it is clear that mixtures of PEO with protonated and deuteriated PMMA cannot be considered as simple binary mixtures. Rigorous analysis of these data would require the use of ternary solution theory as discussed by Benoit et al.[9,42] However, given the relatively small magnitudes of χ_{AB} measured and the experimental inaccuracies it is doubtful that meaningful measures of the three different χ's, i.e., the interaction parameters between PEO and PMMAD, PEO and PMMAH, and PMMAH and PMMAD, could be obtained from these data. It is necessary to examine more closely the scattering from PMMAH and PMMAD above the glass transition temperature of the polymer to ensure thermodynamic equilibrium in order to precisely determine χ_{HD}.

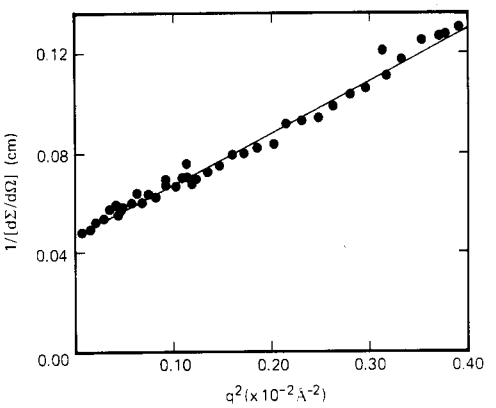

Figure 10. Zimm plot of a 50/50 PMMA/PEO mixture where the PMMA is fully deuteriated. The slope to intercept ratio of these data yields $\langle R_{ap}^2 \rangle$.

Table IV
Apparent Radii of Gyration and Interaction Parameters for PMMAD/PEO Mixtures[a]

PMMAD monomer fraction	$\langle R_{ap}^2 \rangle^{1/2}$, Å	$\chi_{13} \times 10^4$
0.3	71	−2.5
0.50	86	−2.1
0.75	93	−9.5

[a] $u = 0.456$; $v = 0.374$.

A measure of the interaction parameter between PEO and PMMAD can be made from the scattering observed for the PEO/PMMAD mixtures. Recently, Lapp et al.[43] presented a means of measuring the interaction parameter in miscible polymer blends by examining the apparent radius of gyration $\langle R_{ap}^2 \rangle^{1/2}$. By use of their nomenclature,

$$\langle R_{ap}^2 \rangle = \langle R_z^2 \rangle \frac{(1-u)(1+v) + 2\phi_A(u-v)}{1 + u(2\phi_A - 1) - 2\bar{n}_w(1-u^2)\phi_A(1-\phi_A)\chi} \tag{10}$$

where $\langle R_{ap}^2 \rangle^{1/2}$ is the apparent radius of gyration measured for the mixture containing a volume fraction ϕ_A of component A, $\bar{n}_w$ is the average weight-average molecular weight ($\bar{n}_w = \bar{n}_{w,A} + \bar{n}_{w,B}$), and u is the heterogeneity parameter given by $n_{w,A} - n_{w,B}$. The relationship between $\langle R_z^2 \rangle$ and the mean-square radius of gyration of either component is given by

$$\langle R_{z,A}^2 \rangle = \langle R_z^2 \rangle (1+v) \qquad \langle R_{z,B}^2 \rangle = \langle R_z^2 \rangle (1-v) \tag{11}$$

where $v = (n_{z,A} - n_{z,B})/(n_{z,A} + n_{z,B})$. Therefore, if the molecular weight distributions of the two polymers are known and the radius of gyration of only one of the components in the bulk is known, then, by measurement of the apparatus radius of gyration, χ can be obtained from eq 10.

An example of a Zimm analysis to measure $\langle R_{ap}^2 \rangle$ for the 50/50 PEO/PMMA mixture is shown in Figure 10. As can be seen, over a large range in the scattering vector the Zimm plot is linear, thereby permitting an easy measurement of $\langle R_{ap}^2 \rangle$. Values of $\langle R_{ap}^2 \rangle^{1/2}$ determined for the different concentrations of PMMAD in the mixtures are given in Table IV. As can be seen, the apparent radius of gyration increases with the concentration of PMMAD. Use of the radius of gyration determined in pure PMMA and the parameters u and v (shown at the bottom of Table

IV) characterizing the molecular weight distributions of the PEO and PMMA yields the values of χ_{13} shown in Table IV where χ_{13} is the interaction parameter between PEO and PMMAD. Consistent with the values of χ_{AB}, where χ_{AB} is the total interaction parameter of the mixture, χ_{13} is small and comprises a large fraction of the total interaction parameter. Thus, it would be expected that χ_{12}, the interaction parameter between PEO and PMMAH, would be even smaller than the value of χ_{AB} reported in Figure 9. This, in turn, would further reduce the expected melting point depressions in the mixtures and would be more consistent with our previous work.[10]

Conclusions

Small-angle neutron-scattering studies on mixtures of PEO and PMMA have conclusively shown that the interaction parameter for this mixture, χ_{AB}, is negative but very small in magnitude. This result is consistent with previous melting point depression studies. In addition, χ_{AB} was found to depend upon composition, increasing with increasing concentration of PMMA and becoming positive at concentrations of PMMA in excess of 0.8 monomer fraction. The change in sign of χ and the temperature invariance of χ indicate that χ_{AB} is dominated by entropic contributions. Absolute Kratky plots have also shown that the conformation of PMMA in the mixture is identical with that of PMMA in the bulk down to a size scale of ca. 25 Å. At distances ≤25 Å differences in the single-chain scattering function of PMMA are observed in the mixtures. However, experimental precision and slight tacticity differences of the H and D PMMA preclude interpretation of this finding. The results of this study indicate that PEO and PMMA are miscible on the segmental level; however, entropic rather than enthalpic contributions dominate the interactions.

Acknowledgment. We are indebted to Prof. G. C. Alfonso (Universita Genova) and H. Benoit (CRM, Strasbourg) for several enlightening discussions during the course of this work. We are also grateful to F. Bates for his suggestions on the evaluation of the H/D interaction parameter for PMMA. We also thank R. Herbold for the NMR characterization of PMMA and Dr. P. M. Cotts for the measurements of the molecular weight by light-scattering and size-exclusion chromatography. We are also endebted to Drs. M. Bawendi, K. F. Freed, R. S. Porter, and J. M. Lefebvre for making their results available prior to publication. Finally, we would like to acknowledge use of the scattering facility at the National Center for Small Angle Scattering Research at the Oak Ridge National Laboratory.

Registry No. PEO, 25322-68-3; PMMAH, 9011-14-7; PMMAD, 63541-79-7; neutron, 12586-31-1.

References and Notes

(1) Nishi, T.; Wang, T. T. *Macromolecules* **1975**, *8*, 909.
(2) Weeks, N. E.; Karasz, F. E.; MacKnight, W. J. *J. Appl. Phys.* **1977**, *48*, 4068.
(3) Olabisi, O. *Macromolecules* **1975**, *8*, 316.
(4) Kramer, E. J.; Green, P.; Palmstrom, C. J. *Polymer* **1984**, *25*, 473.
(5) Green, P.; Doyle, B. L. *Phys. Rev. Lett.*, in press.
(6) Wendorff, J. H. *J. Polym. Sci., Polym. Lett. Ed.* **1980**, *18*, 439.
(7) Warner, M.; Higgins, J. S.; Carter, A. J. *Macromolecules* **1983**, *16*, 1931.
(8) Hadziioannou, G.; Stein, R. S. *Macromolecules* **1984**, *17*, 567.
(9) Benoit, H.; Benmouna, M. *Macromolecules* **1984**, *17*, 535.
(10) Alfonso, G. C.; Russell, T. P. *Macromolecules* **1986**, *19*, 1143.
(11) Allen, R. D.; McGrath, J. E. *Polym. Prepr. (Am. Chem. Soc., Div. Polym. Chem.)* **1984**, *25*, 9.
(12) Koehler, W. C. *Physica B–C (Amsterdam)*, **1986**, *137*, 320.
(13) Wignall, G. D.; Bates, F. S. *J. Appl. Crystallogr.*, in press.
(14) Hayashi, H.; Flory, P. J.; Wignall, G. D. *Macromolecules* **1983**, *16*, 1328.
(15) Akcasu, A. Z.; Summerfield, G. C.; Jashan, S. N.; Han, C. C.; Kim, C. V.; Yu, H. *J. Polym. Sci., Polym. Phys. Ed.* **1980**, *18*, 863.
(16) Benoit, H.; Koberstein, J. T.; Leibler, L. *Makromol. Chem. Suppl.* **1981**, *4*, 85.
(17) Boue, F.; Nierlich, M.; Leibler, L. *Polymer* **1982**, *23*, 29.
(18) Jashan, S. N.; Summerfield, G. C. *J. Polym. Sci., Polym. Phys. Ed.* **1980**, *18*, 1859, 2415.
(19) de Gennes, P.-G. Scaling Concepts in Polymers; Cornell University Press: Ithaca, NY, 1979.
(20) Buckingham, A. D.; Hentschel, G. H. E. *J. Polym. Sci., Polym. Phys. Ed.* **1980**, *18*, 853.
(21) Bates, F. S.; Wignall, G. D.; Koehler, W. C. *Phys. Rev. Lett.* **1985**, *55*, 2425.
(22) Bates, F. S.; Wignall, G. D. *Macromolecules* **1986**, *19*, 932.
(23) Bates, F. S.; Dierker, S. B.; Wignall, G. D. *Macromolecules* **1986**, *19*, 1938.
(24) Ullman, R. *J. Polym. Sci., Polym. Phys. Ed.* **1985**, *23*, 1477.
(25) Dettenmeier, M.; Maconnachie, A.; Higgins, J. S.; Kausch, H. H.; Nguyen, T. Q. *Macromolecules* **1986**, *19*, 773.
(26) O'Reilly, J. M.; Teegarden, D. M.; Wignall, G. D. *Macromolecules* **1985**, *18*, 2747.
(27) Flory, P. J. Statistical Mechanics of Chain Molecules; Interscience: New York, 1969.
(28) Sundararajan, P. R.; Flory, P. J. *J. Am. Chem. Soc.* **1974**, *96*, 5025.
(29) Jenkins, R.; Porter, R. S. *Polymer* **1982**, *23*, 105.
(30) Kirste, R. G.; Kratky, O.; Ibel, K. *Phys. Chem.* **1962**, *31*, 363.
(31) Kirste, R. G.; Wunderlich, W. *Makromol. Chem.* **1964**, *73*, 240.
(32) Kirste, R. G.; Kruse, W. A.; Ibel, K. *Polymer* **1975**, *16*, 120.
(33) Yamaguchi, S.; Hayashi, H.; Hamada, F.; Nakajima, A. *Macromolecules* **1984**, *17*, 2131.
(34) Yoon, D. Y.; Flory, P. J. *Polymer* **1975**, *16*, 645.
(35) Yoon, D. Y.; Flory, P. J. *Macromolecules* **1975**, *9*, 294, 299.
(36) Vacatello, M.; Flory, P. J. *Polym. Commun.* **1984**, *25*, 258.
(37) Benoit, H.; Benmouna, J. *Polymer* **1984**, *25*, 1059.
(38) Lefebvre, J. M.; Porter, R. S.; Wignall, G. D., manuscript in preparation.
(39) Lefebvre, J. M.; Porter, R. S.; Wignall, G. D.; Russell, T. P., unpublished results.
(40) Bawendi, M.; Freed, K. F., submitted for publication in *J. Chem. Phys.*
(41) Bates, F. S.; Wignall, G. D. *Phys. Rev. Lett.* **1986**, *57*, 1429.
(42) Benoit, H.; Wu, W.; Benmouna, M.; Mozer, B.; Bauer, B.; Lapp, A. *Macromolecules* **1985**, *18*, 986.
(43) Lapp, A.; Picot, C.; Benoit, H. *Macromolecules* **1985**, *18*, 2437.